

---

## Review of NEUT

---

Jun KAMEDA

*Kamioka Observatory, Institute for Cosmic Ray Research, University of Tokyo,  
Higashi-Mozumi, Kamioka City Hida-shi, Gifu 506-1205, Japan*

---

### Abstract

I reviewed NEUT, which is a simulation program for neutrino interaction.

### 1. Introduction

NEUT is the simulation program originally developed and used in Kamiokande experiment, and continuously updated and used in Super-Kamiokande and K2K experiments. NEUT is used for the study of atmospheric neutrinos and accelerator neutrinos, and covers from several 10 MeV to TeV region. NEUT also simulates the secondary particles in oxygen nuclei.

### 2. Neutrino Interaction

Neutrino interactions in the energy region concerning to the Super-Kamiokande and K2K experiment are categorized into the following types:

1. NC elastic / CC quasi elastic scattering off nucleon ( $\nu + N \rightarrow l + N'$ )
2. CC/NC single meson production via resonances ( $\nu + N \rightarrow l + N' + \text{meson}$ )
3. CC/NC deep inelastic scattering ( $\nu + N \rightarrow l + N' + \text{hadrons}$ )
4. CC/NC coherent pion production ( $\nu + {}^{16}\text{O} \rightarrow l + {}^{16}\text{O} + \pi$ )

where  $l$  represents a charged or a neutral lepton,  $N$  and  $N'$  represents nucleons, respectively.

#### 2.1. Elastic and Quasi elastic scattering ( $\nu + N \rightarrow l + N'$ )

The cross section is based on Llewellyn Smith's theory [1]. The amplitude of this process is described by the product of the hadron and lepton weak currents:

$$T = \frac{G_F}{\sqrt{2}} \bar{u}_l(k_2) \gamma^\mu (1 - \gamma_5) u_\nu(k_1) \langle N'(p_2) | J_\mu^{\text{hadron}} | N(p_1) \rangle \quad (1)$$

where  $G_F$  is the Fermi coupling constant,  $p_1(p_2)$  is a initial(final) nucleon 4-momentum, and  $k_1(k_2)$  is a initial(final) lepton 4-momentum, respectively. The hadronic weak current,  $J^{\text{hadron}}$ , is expressed as:

$$\langle N' | J_\mu^{\text{hadron}} | N \rangle = \cos \theta_c \bar{u}_{N'}(p_2) \left[ \gamma_\mu F_V^1(q^2) + \frac{i\sigma_{\mu\nu} q^\nu \xi F_V^2(q^2)}{M} + \gamma_\mu \gamma_5 F_A(q^2) \right] u_N(p_1) \quad (2)$$

where  $F_V^1(q^2)$  and  $F_V^2(q^2)$  are the vector form factor,  $F_A(q^2)$  is the axial vector form factors,  $q \equiv k_1 - k_2$  is a 4-momentum transfer,  $M$  is the target nucleon mass,  $\theta_c$  is the Cabibbo angle,  $\xi \equiv \mu_p - \mu_n = 3.71$ , respectively.  $F_V^1(q^2)$  and  $F_V^2(q^2)$  are written in terms of the electric and magnetic form factors,  $G_E$  and  $G_M$ :

$$\begin{aligned} F_V^1(q^2) &= \left(1 - \frac{q^2}{4M^2}\right)^{-1} \left[ G_E(q^2) - \frac{q^2}{4M^2} G_M(q^2) \right] \\ \xi F_V^2(q^2) &= \left(1 - \frac{q^2}{4M^2}\right)^{-1} [G_E(q^2) - G_M(q^2)] \end{aligned} \quad (3)$$

The electric and magnetic form factor have dipole forms which are experimentally determined by electron scattering experiments:

$$G_E(q^2) = (1 + \xi)^{-1} G_M(q^2) = \frac{1}{\left(1 - \frac{q^2}{M_V^2}\right)^2} \quad (4)$$

where  $M_V$  is vector mass which is set to be 0.84 GeV/ $c^2$  in NEUT.  $F_A$  is assumed to have a dipole form:

$$F_A(q^2) = -\frac{1.23}{\left(1 - \frac{q^2}{M_A^2}\right)^2} \quad (5)$$

where  $M_A$  is the axial vector mass, and we adopt 1.1 GeV/ $c^2$  in NEUT.  $F_A(0) = -1.23$  is obtained from neutron  $\beta$  decay experiments [2]. The differential cross sections  $d\sigma/dq^2$  are written as:

$$\frac{d\sigma^{\nu(\bar{\nu})}}{dq^2} = \frac{M^2 G_F^2 \cos^2 \theta_c}{8\pi E_\nu^2} \left[ A(q^2) \mp B(q^2) \frac{s-u}{M^2} + C(q^2) \frac{(s-u)^2}{M^4} \right] \quad (6)$$

where  $s$  and  $u$  are Mandelsam variables which are defined to be  $s \equiv (k_1 + p_1)^2$  and  $u \equiv (k_1 - p_1)^2$ ,  $E_\nu$  is a neutrino energy,  $m$  is an outgoing lepton mass, respectively.  $A(q^2)$ ,  $B(q^2)$ , and  $C(q^2)$  are written as follows:

$$A(q^2) = \frac{m^2 - q^2}{4M^2} \left[ \left(4 - \frac{q^2}{M^2}\right) |F_A|^2 - \left(4 + \frac{q^2}{M^2}\right) |F_V^1|^2 \right]$$

$$\begin{aligned}
 & - \frac{q^2}{M^2} |\xi F_V^2|^2 \left( 1 + \frac{q^2}{4M^2} \right) - \frac{4q^2 F_V^1 \xi F_V^2}{M^2} - \frac{m^2}{M^2} \left( (F_V^1 + \xi F_V^2)^2 + |F_A|^2 \right) \Big] \\
 B(q^2) &= \frac{q^2}{M^2} (F_A(F_V^1 + \xi F_V^2)) \\
 C(q^2) &= \frac{1}{4} \left( |F_A|^2 + |F_V^1|^2 - \frac{q^2}{4M^2} |\xi F_V^2|^2 \right) \tag{7}
 \end{aligned}$$

Fig. 2.1. shows the calculated cross section and experimental data of quasi-elastic scattering.

We consider the Fermi motion of the target nucleon and the Pauli blocking effect. We assume the simple fermi gas model with the fermi surface  $P_f = 225\text{MeV}/c$ . And also we consider the nuclear potential with 27 MeV depth. The Pauli blocking effect is considered by requiring the outgoing nucleon's momentum is larger than the Fermi surface momentum. Fig. 2.1. shows the calculated cross sections with free proton and bound nucleon in oxygen nuclei. The pauli blocking effect makes the cross sections smaller about 30% at  $E_\nu$  is 1GeV.

NC elastic cross sections are calculated by multipling factors to CC quasi elastic scattering cross sections:

$$\sigma(\nu p \rightarrow \nu p) = 0.153 \times \sigma(\nu n \rightarrow e^- p) \tag{8}$$

$$\sigma(\bar{\nu} p \rightarrow \bar{\nu} p) = 0.218 \times \sigma(\bar{\nu} p \rightarrow e^+ n) \tag{9}$$

$$\sigma(\nu n \rightarrow \nu n) = 1.5 \times \sigma(\nu p \rightarrow \nu p) \tag{10}$$

$$\sigma(\bar{\nu} n \rightarrow \bar{\nu} n) = 1.0 \times \sigma(\bar{\nu} p \rightarrow \bar{\nu} p) \tag{11}$$

These numerical factors are taken from Ref. [3, 4].

## 2.2. Single meson productions via baryon resonances ( $\nu + N \rightarrow l + N' + \text{meson}$ )

The single-meson productions via resonances are the dominant hadron production processes in the region where the invariant mass of the hadron system ( $W$ ) is less than about  $2.0 \text{ GeV}/c^2$ .

We simulate the single-meson productions via resonances based on Rein and Sehgal's theory [10]. This theory was originally developed for single-pion productions. We extended their theory to  $\eta$  and  $K$  meson productions. In this theory, single-meson production is considered in 2 steps:

$$\begin{aligned}
 \text{Resonance production} & \quad \nu + N \rightarrow l(\nu) + N^* \\
 \text{Resonance decay} & \quad N^* \rightarrow N' + \pi(\eta, K)
 \end{aligned}$$

where  $N^*$  is a baryon resonance,  $N$  and  $N'$  are nucleons, and  $l$  is a outgoing lepton. The amplitude of a baryon excitation is described as:

$$T(\nu N \rightarrow l N^*) = \frac{G_F}{\sqrt{2}} \bar{u}_l \gamma^\mu (1 - \gamma_5) u_\nu \langle N^* | J_\mu^h | N \rangle \tag{12}$$

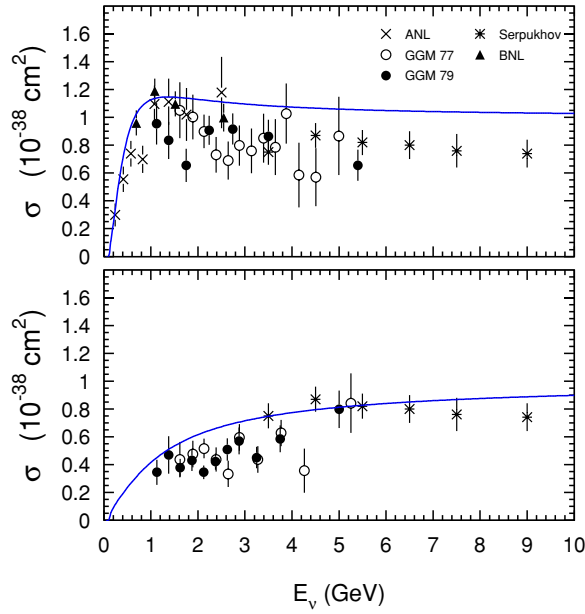


**Fig 1.** Cross section for (a)  $\nu_\mu + n \rightarrow \mu^- + p$  interaction and (b)  $\bar{\nu}_\mu + p \rightarrow \mu^+ + n$  interaction. Solid lines show our calculation and points show experimental data from ANL 12' [5], Gargamelle [6, 7], BNL 7' [8] bubble chambers and a spark chamber experiment at Serpukhov [9].

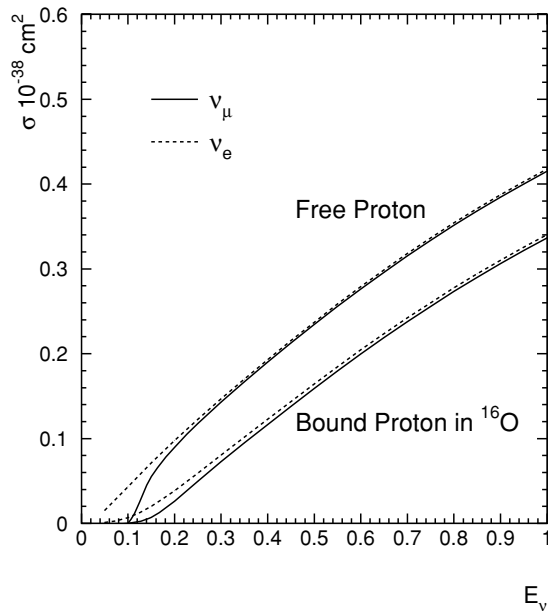


**Fig 2.** Calculated QE cross sections. Upper two lines show the cross sections for free proton, and lower two lines show the cross sections for bound proton in oxygen.

where  $\langle N^* | J_\mu^h | N \rangle$  is the weak hadron current for this process. The matrix element of the hadron current is calculated by the FKR(Feynman,Kislinger,Ravndal) baryon model [11]. The amplitude of the resonance decay,  $\langle N\pi | N^* \rangle$ , is expressed by Breit-Wigner formula with experimentally measured decay width and branching ratio of each resonance [49].

The differential cross section is written as:

$$\frac{d^2\sigma}{dq^2 dW} = \frac{1}{32\pi M E_\nu^2} \cdot \frac{1}{2} \left| \sum_{j,spin} T(\nu N \rightarrow l N_j^*) \cdot \sqrt{\chi_E} \cdot \left( sign(N_j) \sqrt{\frac{\Gamma_j}{2\pi}} \cdot \frac{1}{W - M_j + i\frac{\Gamma_j}{2}} \right) \right|^2, \quad (13)$$

where  $N_j^*$  represents j's baryon resonance,  $E_\nu$  is neutrino energy,  $\chi_E$  is the branching ratio of  $N_j^*$  to  $N'+$  meson,  $M_j$  is  $N_j^*$ 's mass,  $\Gamma_j$  is the total decay width of  $N_j^*$ ,  $sign(N_j)$  is a sign of the decay amplitude of  $N_j^*$ , respectively. The  $sign(N_j)^*$  is a sign of the decay amplitude of  $N_j^*$  which is lost in the experimentally measured decay width. This factor is calculated by the FKR model, and added to the decay amplitude in order to consider the interference effects of the neighboring resonances correctly. Summation in Eq.(13) is over all relevant resonances and their spin. In NEUT, a region where  $W < 2.0$  GeV/ $c^2$  is covered and 18 resonances ( $\Delta(1232)$ ,  $N^*(1440)$ , etc.) are taken into account. The interferences of the resonances are correctly considered in Eq.(13).

In the Rein and Sehgal's methods, the final kinematics of the hadron system is determined so that the effects of the polarization of the produced resonances and the interference are properly considered. In NEUT, we employ their detailed methods only for  $\Delta(1232)$ , and we simply assume that the mesons are emitted isotropically in resonance rest frame for other resonances.

It is known that a baryon resonance in a nucleus can disappear without meson emissions via the following interaction:



where  $N^*$  is a baryon resonance, and  $N, N', N''$  are nucleons. The rate of the interactions are estimated from theoretical calculation [12]. We assume that 20% of resonances in  $^{16}\text{O}$  disappear without meson emissions.

Fermi momentum of nucleons are considered as in the quasi elastic interaction case. The Pauli blocking effect on the nucleon from the baryon resonances decay is also taken into account. Figs. 2.2. show the calculated cross sections and experimental data for CC  $\nu_\mu$  interaction.

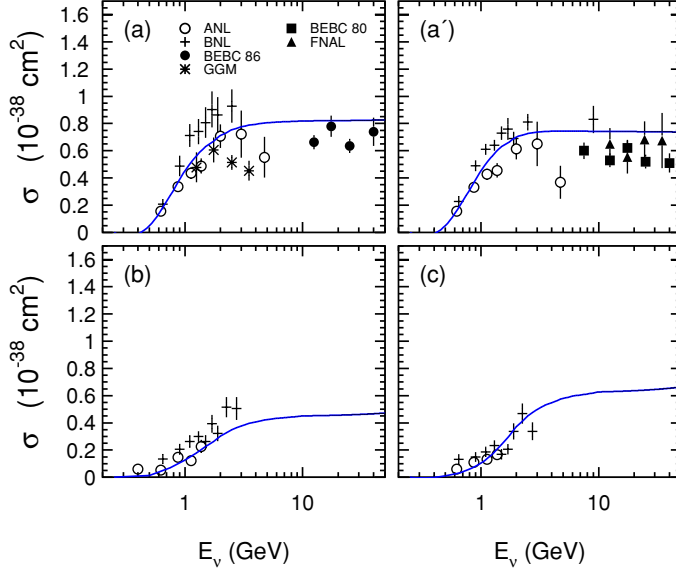


**Fig 3.** Total cross sections for CC  $\nu_\mu$  single pion productions. (a)  $\nu_\mu + p \rightarrow \mu^- + p + \pi^+$  (a')  $\nu_\mu + p \rightarrow \mu^- + \Delta^{++}$  ( $\nu_\mu + p \rightarrow \mu^- + p + \pi^+$  with  $W < 1.4$  GeV/ $c^2$  cut) (b)  $\nu_\mu + n \rightarrow \mu^- + p + \pi^0$  (c)  $\nu_\mu + n \rightarrow \mu^- + n + \pi^+$ . Solid lines show the calculations used in our MC simulation, and points show the experimental data taken from bubble chamber experiments: ANL [13], BNL [14], BEBC [15, 16], Gargamelle [17], FNAL [18].

### 2.3. Coherent pion production off $^{16}\text{O}$ ( $\nu + ^{16}\text{O} \rightarrow l(\nu) + ^{16}\text{O} + \pi$ )

Coherent pion production is a neutrino interaction with a nucleus as a whole. Differential cross section of coherent pion production is calculated by Rein & Sehgal [23]:

$$\begin{aligned} \frac{d^3\sigma}{dx dy dt} &= \frac{G_F^2 M}{2\pi^2} f_\pi^2 A^2 E_\nu (1-y) \frac{1}{16\pi} [\sigma_{tot}^{\pi^0 N}(E_\nu y)]^2 \left( 1 + \left( \frac{\text{Re}(f_{\pi N}(0))}{\text{Im}(f_{\pi N}(0))} \right)^2 \right) \\ &\times \left( \frac{M_A^2}{M_A^2 + Q^2} \right)^2 \exp\left(-\frac{1}{3} R^{2/3} |t|\right) F_{abs} \end{aligned} \quad (15)$$

where  $x$  and  $y$  are the Bjorken parameters,  $t$  is a square of 3-momentum transfer,  $f_\pi$  is pion decay constant ( $=0.93m_\pi$ ),  $f_{\pi N}$  is the pion-nucleon scattering amplitude,  $A$  is the atomic number of oxygen ( $=16$ ),  $M_A$  is axial vector mass,  $M$  is the nucleon mass,  $R$  is the radius of oxygen nuclear,  $\sigma_{tot}^{\pi^0 N}$  is the averaged cross section of pion-nucleon scattering,  $F_{abs}$  is a  $t$ -independent factor representing the effect of pion absorption in the nucleus, respectively. In K2K experiment, we employ the calculation by Marteau et al. [24]. for the total cross section. Figs. 4 shows the calculated cross sections.

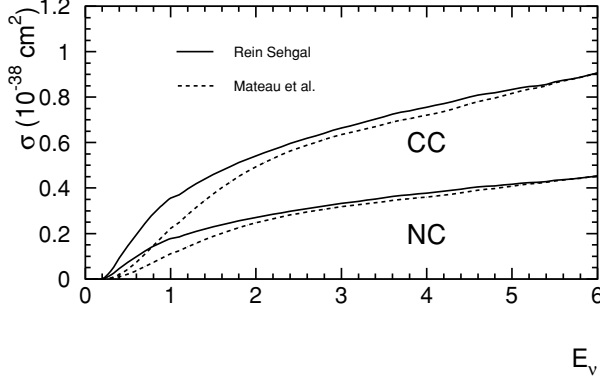


**Fig 4.** Cross section of coherent pion production. Upper two lines are for CC interaction, lower two lines are for NC interaction. Solid line is calculation by Rein and Sehgal, broken lines by Marteau et al.

#### 2.4. Deep inelastic scattering ( $\nu + N \rightarrow l(\bar{\nu}) + N' + \text{hadrons}$ )

The differential cross section for the deep inelastic scattering is described as follows [25]:

$$\begin{aligned}
 \frac{d^2\sigma^{\nu(\bar{\nu})}}{dx dy} &= \frac{G_F^2 M E_\nu}{\pi} \left( \left( 1 - y + \frac{y^2}{2} + C_1 \right) F_2'(x, q^2) \right. \\
 &\quad \left. \pm y \left( 1 - \frac{y}{2} + C_2 \right) (x F_3'(x, q^2)) \right), \\
 C_1 &= \frac{y m^2}{4 M E_\nu x} - \frac{x y M}{2 E_\nu} - \frac{m^2}{4 E_\nu^2} - \frac{m^2}{2 M E_\nu x}, \\
 C_2 &= -\frac{m^2}{4 M E_\nu x} \\
 F_2'(x, q^2) &= \frac{q^2}{q^2 + 0.188} F_2(x', q^2), \\
 x F_3'(x, q^2) &= \frac{q^2}{q^2 + 0.188} x F_3(x', q^2), \\
 x' &= x(q^2 + 0.624)/(q^2 + 1.735x)
 \end{aligned} \tag{16}$$

where  $x, y$  are Bjorken parameters,  $F_2(x, q^2)$  and  $x F_3(x, q^2)$  are the nucleon structure functions,  $M$  and  $m$  are the target nucleon mass and the outgoing lepton mass, respectively. We adopt GRV94 parton distribution function (PDF) [27, 28] for the calculation of  $F_2$  and  $x F_3$ . We also include corrections for GRV94 PDF in small  $q^2$  region which is taken from [26]. In order to keep the consistency with the other interaction modes, we consider this interaction in the region where  $W > 1.3 \text{ GeV}/c^2$ , and we require that the number of produced pions via the deep inelastic scattering should be greater than 1 for a region  $1.3 \text{ GeV}/c^2 < W < 2.0 \text{ GeV}/c^2$ .

The final kinematics of the hadron system is obtained in 2 different ways. For a region where  $1.3 \text{ GeV}/c^2 < W < 2.0 \text{ GeV}/c^2$ , the produced mesons are assumed to be pions. We determine the pion multiplicity from the measured charged

pion multiplicity by FNL 7-foot hydrogen bubble chamber experiment [33]:

$$\langle n_{\pi^\pm} \rangle = (0.06 \pm 0.06) + (1.22 \pm 0.03) \ln(W^2) \quad (17)$$

where  $\langle n_{\pi^\pm} \rangle$  is the mean multiplicity of charged pions. Assuming  $\langle n_{\pi^+} \rangle = \langle n_{\pi^-} \rangle = \langle n_{\pi^0} \rangle$ , the mean multiplicity of pion  $\langle n_\pi \rangle$  is described as:

$$\langle n_\pi \rangle = 0.09 + 1.83 \ln(W^2) \quad (18)$$

For individual Monte Carlo events, the pion multiplicity are determined using KNO(Koba-Nielsen-Olesen) scaling which describes the pion multiplicity distribution with the mean multiplicity  $\langle n_\pi \rangle$ . We also consider the forward-backward asymmetry of pion multiplicity ( $n_\pi^F/n_\pi^B$ ) in the hadronic center of the mass system [29]:

$$\frac{n_\pi^F}{n_\pi^B} = \frac{0.35 + 0.41 \ln(W^2)}{0.5 + 0.09 \ln(W^2)} \quad (19)$$

where forward means the direction of the hadronic system in the laboratory frame. For a region where  $W > 2.0 \text{ GeV}/c^2$ , final kinematics of hadrons is determined by JETSET 7.4 package [32] which is commonly used in high energy physics. The package considers other particles productions than pions ( $K, \eta, \rho$ , etc.).

For NC deep inelastic scattering, differential cross sections are calculated by multiplying the factors to CC cross sections estimated from experimental results shown in Ref. [30, 31]:

$$\frac{\sigma(\nu N \rightarrow \nu X)}{\sigma(\nu N \rightarrow \mu^- X)} = \begin{cases} 0.26 & (E_\nu \leq 3\text{GeV}) \\ 0.26 + 0.04 \times \frac{E_\nu - 3}{3} & (3 < E_\nu < 6\text{GeV}) \\ 0.30 & (E_\nu \geq 6\text{GeV}) \end{cases} \quad (20)$$

$$\frac{\sigma(\bar{\nu} N \rightarrow \bar{\nu} X)}{\sigma(\bar{\nu} N \rightarrow \mu^+ X)} = \begin{cases} 0.39 & (E_\nu \leq 3\text{GeV}) \\ 0.39 - 0.02 \times \frac{E_\nu - 3}{3} & (3 < E_\nu < 6\text{GeV}) \\ 0.37 & (E_\nu \geq 6\text{GeV}) \end{cases} \quad (21)$$

### 3. Nuclear effects

We consider the interactions of produced mesons ( $\pi, K, \eta$ ) in a  $^{16}\text{O}$  nucleus in our simulation. In K2K experiments, interactions of nucleons are also considered.

For pions, inelastic scattering, charge exchange, and absorption are considered. The cross section of each interaction is calculated by the model of L.Salcedo *et al.*[46]. The momentum and angular distribution of the scattered pions are determined from the results of the phase shift analysis using the experimental results



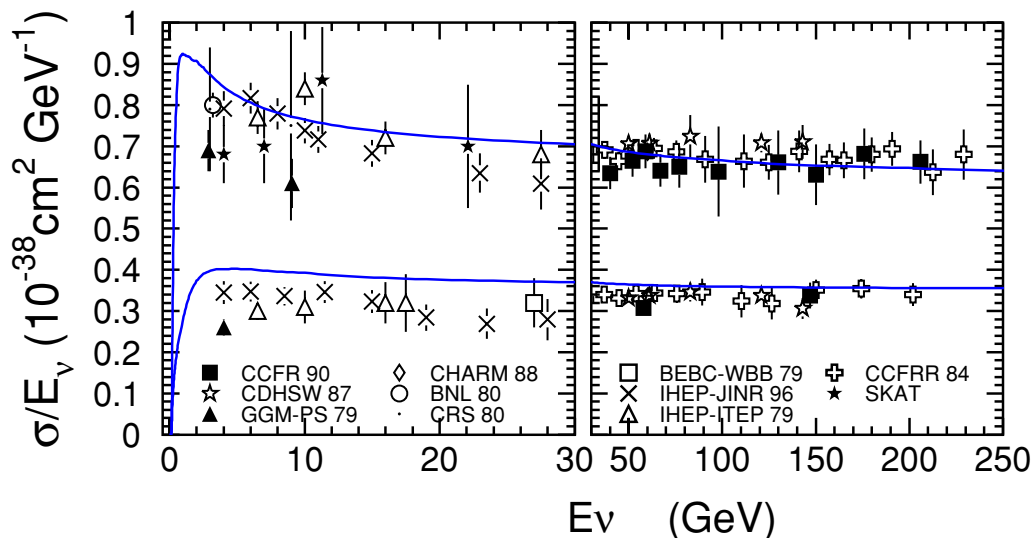


**Fig 5.** Cross sections for CC inclusive interactions on iso-scalar target for (a)  $\nu_\mu + N \rightarrow \mu^- + X$ , and (b)  $\bar{\nu}_\mu + N \rightarrow \mu^+ + X$ . Solid lines are the sum of the cross sections of all interaction modes described in the text, and dashed lines show  $\pm 10\%$  scaled lines. Points show experimental data from CCFR [34], CDHSW [35], Gargamelle [36, 37], CHARM [38], BNL [39], CRS [40], BEBC-WWB [41], IHEP-JINR [42], IHEP-ITEP [43], CCFRR [44], SKAT [45].

on  $\pi$ - $N$  scattering [47]. We consider the Pauli blocking effects in  $\pi$ - $N$  scattering in  $^{16}\text{O}$  by requiring that the momentum of scattered nucleon should be larger than fermi surface momentum. Figs. 6 shows the calculated  $\pi$ - $^{16}\text{O}$  scattering cross section compared with the experimental results [48].

For kaons, elastic scattering and charge exchange are considered. The cross sections of the interactions are based on the measured  $K^\pm N$  scattering data from Ref. [49]. The cross sections for  $K^0$  and  $\bar{K}^0$  are obtained from  $K^\pm N$  results assuming the isospin symmetry.

For  $\eta$ , interactions via baryon resonances  $\eta + N \rightarrow N^* \rightarrow N + X$  are considered, where  $X$  is either  $\eta$ ,  $\pi$ , or  $\pi\pi$ .  $N(1535)$  and  $N(1650)$  are the relevant resonances concerning about  $\eta$  interactions [49]. Cross section is given by Breit Wigner formula. The direction of the scattered  $\eta$  meson is assumed to be isotropic in the resonance rest frame. For nucleons, elastic scattering and resonances productions are simulated. The cross sections are calculated based on the experimental data. NEUT also simulate gammas emission from the de-excitation of nuclei. This calculation is based on [50].

For K2K experiments, NEUT is used for Fe and Carbon target. For Fe target, we changed fermi surface momentum to 250 MeV/c, and no change for Carbon. The proton/neutron ratio is taken into account. Nuclear effects are not

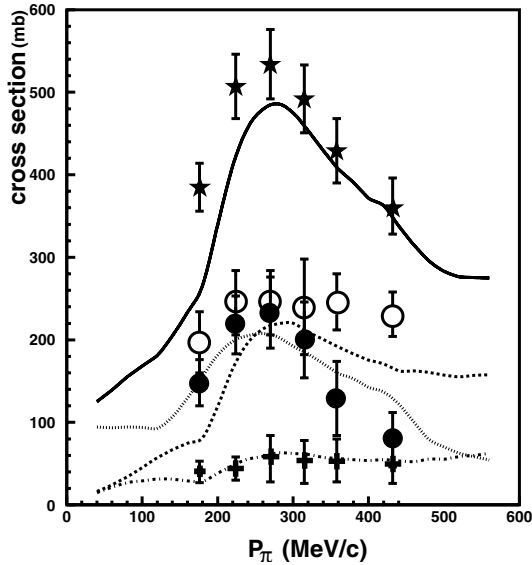


**Fig 6.** The calculated cross sections of  $\pi-^{16}\text{O}$  interaction compared with the experimental data [48]. The lines show the calculated cross sections. The stars (solid line) shows the total cross section, the white circles (broken line) show the inelastic scattering cross section the black circles (dashed line) show the absorption cross section, and the crosses (dashed dotted line) show the charge exchanges cross section, respectively.

modified for C and Fe, but the effects of this approximation is estimated to be small in K2K experiments.

#### 4. Summary

I reviewed NEUT program. I presented the details of the model in NEUT. NEUT is made with available models and experimental data. K2K front detectors now have a huge amount of neutrino interaction data, and it will give a good information for neutrino interaction models.

#### References

- [1] C.H.Llewellyn Smith, Phys. Rep. 3, 261 (1972)
- [2] Particle data group, Rev. Mod. Phys. 52 (1980) S1
- [3] C.H.Albright et al., Phys. Rev. D14 (1976) 1780
- [4] K.Abe et al., Phys. Rev. Lett. 56 (1986) 1107
- [5] S.Barish et al., Phys. Rev. D16 (1977) 3103
- [6] S.Bonetti et al., Nuovo Cimento 38 (1977) 260
- [7] M.Pohl et al., Nuovo Cimento 26 (1979) 332, N.Arimenise et al., Nucl. Phys. B152 (1979) 365
- [8] A.S.Vovenko et al., Yad. Fiz.30 (1979) 1014
- [9] S.Belikov et al., Z. Phys. 320 (1985) 625
- [10] D.Rein and L.M.Sehgal, Ann. of Phys. 133 (1981) 1780
- [11] R.Feynman et al., Phys. Rev. D3 (1971) 2706
- [12] M.Hirata et al., Ann. Phys. (N.Y.) 108 (1977) 116
- [13] G.Radecky et al., Phys. Rev. D25 (1982) 116

- [14] T.Kitagaki et al., Phys. Rev. D34 (1986) 2554
- [15] P.Allen et al., Nucl. Phys. B264 (1986) 221
- [16] P.Allen et al., Nucl. Phys. B176 (1980) 269
- [17] W.Lerche et al., Phys. Lett. 4 (1978) 510
- [18] J.Bell et al., Phys. Rev. Lett. 15 (1978) 1008
- [19] D.Allisia et al., Ann. Phys. 1983
- [20] S.J.Barish et al., Phys. Lett. B91 (1980) 161
- [21] M.Derrick et al., Phys. Rev. D23 (1981) 569
- [22] H.Grabosch et al., Z. Phys. C41 (1989) 527
- [23] D.Rein and L.M.Sehgal, Nucl. Phys B233 (1983) 29
- [24] J.Marteau *et al.*, Nucl. Inst. and Meth., A451 (2000) 76
- [25] C.H.Albright, C.Jarlskog, Nucl Phys. B84 (1975) 467
- [26] A.Bodek and U.K.Yank, Nucl Phys. B112 (2002) 70
- [27] M.Glück, E.Reya, and A. Vogt, Z. Phys. D57 (1995) 433
- [28] H.Plothow-Besch CERN Program Library W5051 (1995)
- [29] S.Barlag et al., Z.Phys. C11 (1982) 283
- [30] Paul Musset and Jean-Pierre Vialle, Phys. Rep. C39 (1978) 1
- [31] J.E.Kim et al., Rev. Mod. Phys. 53 (1981) 211
- [32] T.Sjöstrand et al., CERN-TH-7112-93 (1994)
- [33] S.J.Barish et al., Phys. Rev. D17 (1978) 1
- [34] P.S.Auchincloss et al., Z. Phys. C48 (1990) 411
- [35] P.Berger et al., Z. Phys. C35 (1987) 443
- [36] S.Campolillo et al., Phys. Lett. 84B (1979) 281
- [37] O.Erriquez et al., Phys. Lett. 89B (1979) 309
- [38] J.V. Allaby et al., Z. Phys. C38 (1988) 403
- [39] N.J.Baker et al., Phys. Rev. D25 (1982) 617
- [40] C. Baltay et al., Phys. Rev. Lett. 44 (1980) 916
- [41] D.C.Colley et al., Z. Phys. C2 (1979) 187
- [42] V.B. Anikeev et al., Z. Phys. C70 (1996) 39
- [43] A.S.Vovenko et al., Yad. Fiz. 30 (1979) 187
- [44] D.B.MacFarlane et al., Z. Phys. C26(1984) 1
- [45] D.S.Baranov et al., Phys. Lett. 81B (1979) 255
- [46] L.Salcedo et al., Nucl. Phys. A484 (1998) 79
- [47] G.Rowe et al., Phys. Rev. C18 (1978) 584
- [48] C.Ingram et al., Phys. Rev. C27 (1983) 1578
- [49] Particle Data Group, *Review of Particle Physics* Euro. Phys. Journal C15 (2000)
- [50] H.Ejiri, Phys. Rev C48 (1993) 1442